Circular Dichroism Spectra and Electrophoretic Mobility Shift Assays Show That Human Replication Protein A Binds and Melts Intramolecular G-Quadruplex Structures[†,‡]

Jun-Huei Fan,[§] Elena Bochkareva,[||] Alexey Bochkarev,[||,⊥] and Donald M. Gray*[,§]

Department of Molecular and Cell Biology, Mail Stop FO31, The University of Texas at Dallas, 800 West Campbell Road, Richardson, Texas 75080, Banting and Best Department of Medical Research and Department of Medical Genetics and Microbiology, University of Toronto, 100 College Street, University of Toronto, Toronto, Ontario M5G 1L6, Canada, and Department of Biochemistry and Molecular Biology, University of Oklahoma Health Sciences Center, Oklahoma City, Oklahoma 73190

Received August 14, 2008; Revised Manuscript Received December 6, 2008

ABSTRACT: Noncanonical DNA structures such as G-quadruplexes might obstruct the binding of hRPA, compromising the accuracy of replication, and be a source of genomic instability. In this study, circular dichroism (CD) and electrophoretic mobility shift assay (EMSA) experiments were used to show that hRPA can bind and melt nontelomeric, intramolecular DNA G-quadruplexes under physiologically germane conditions. EMSA results show that hRPA binds to a 58-mer that includes an embedded quadruplex with an affinity equal to or greater than to nonquadruplex forming 58-mers. Moreover, hRPA binds to a 26-mer purine-rich quadruplex-forming sequence with an affinity indistinguishable from that for binding to the complementary pyrimidine-rich sequence. Under the same conditions, hRPA does not have significant affinity for binding to the duplex formed from the two sequences. Thus, DNA secondary structures can significantly modulate the binding affinity of hRPA over and above its known preference for pyrimidine-rich single-stranded sequences, so that at least some intramolecular G-quadruplex structures may not inhibit hRPA binding during DNA replication. CD spectral changes in combination with EMSA titrations suggest that one hRPA heterotrimer is sufficient to form a stable complex with an unfolded 26-mer G-quadruplex prior to the binding of a second hRPA molecule.

Replication protein A (RPA) is a heterotrimeric single-stranded DNA (ssDNA)[1] binding protein (SSB) that plays fundamental roles in eukaryotic DNA replication, recombination, and repair (*1–4*). The human RPA has three subunits of ~70, 32, and 14 kDa (hRPA70, hRPA32, and hRPA14, respectively) (*1, 2*). The heterotrimer contains four main DNA-binding domains that are of the OB-fold type (*5*), analogous to the OB-fold domains in prokaryotic SSBs such as the *Escherichia coli* SSB (*6*) and g5p of Ff phages (*7*). Domains A, B, and C reside in hRPA70, and domain D is in hRPA32 (*3, 4, 8*). A sequential mode of binding is generally accepted in which domains A, B, and C contact 12−23 nt of DNA and domain D is needed to bind 23−27 nt (*9, 10*). A low-affinity complex that involves only the A and B domains contacting 8−10 nt has also been reported (*11*).

Interactions of RPA with telomeric G-quadruplexes have been of interest because hRPA helps prevent accumulation of telomeric DNA in certain cancer cells (*12*), and scRPA is involved in maintaining telomerase activity in yeast (*13, 14*). RPA-like SSBs are important in regulating yeast telomere homeostasis (*15–18*). Interactions of RPA with nontelomeric quadruplexes are also of interest in that the indiscriminate formation of quadruplex structures could be disruptive of normal DNA replication. In fact, Burge et al. (*19*) have found more than 375000 nonoverlapping sequences in the human genome with quadruplex forming potential. Thus, it is important to investigate the binding and destabilization of nontelomeric G-quadruplex sequences by hRPA.

[†] Support was provided by Grant AT-503 from the Robert A. Welch Foundation.

[‡] This work was performed by J.-H. F. in partial fulfillment of the requirements for the Ph.D. degree in the Department of Molecular and Cell Biology, The University of Texas at Dallas.

* To whom correspondence should be addressed. E-mail: dongray@utdallas.edu. Phone: (972) 883-2513. Fax: (972) 883-2409.

[§] The University of Texas at Dallas.

[||] University of Toronto.

[⊥] University of Oklahoma Health Sciences Center.

[1] Abbreviations: buffer A, 500 mM NaCl, 20 mM sodium phosphate, 5 mM imidazole, 10 μM $ZnCl_2$, 1 mM dithiothreitol, and 3% (v/v) glycerol; CD, circular dichroism; EDTA, ethylenediaminetetraacetic acid; EMSA, electrophoretic mobility shift assay; DSSP, definition of the secondary structure of proteins; DTT, dithiothreitol; ε_{260} or ε_{280}, extinction coefficient at 260 or 280 nm, respectively, in units of M^{-1} cm^{-1}; FRET, fluorescence resonance energy transfer; OB-fold, oligonucleotide/oligosaccharide binding fold; g5p, gene 5 protein of Ff filamentous phages; hRPA, human replication protein A; hRPA binding buffer, 200 mM KCl, 20 mM Tris-HCl (pH 7.4), 10 μM $ZnCl_2$, 1 mM dithiothreitol, and 1.5 mM $MgCl_2$; K_a, apparent binding affinity; nt, nucleotide; P/S ratio, molar concentration ratio of hRPA protein to DNA strand; RT, room temperature; scRPA, *Saccharomyces cerevisiae* replication protein A; SDS−PAGE, sodium dodecyl sulfate−polyacrylamide gel electrophoresis; SELEX, systematic evolution of ligands by exponential enrichment; SSB, single-stranded DNA binding protein; ssDNA, single-stranded DNA; TBE buffer, 90 mM Tris-HCl (pH 7.4), 20 mM boric acid, and 2 mM EDTA; TBST buffer, 50 mM Tris-HCl (pH 7.4), 100 mM NaCl, and 0.05% (v/v) Tween 20; T_m, melting temperature; Tris, tris(hydroxymethyl)aminomethane.

10.1021/bi801538h CCC: $40.75 © 2009 American Chemical Society
Published on Web 01/15/2009

Most published studies on RPA binding have been conducted with homopolymeric oligodeoxynucleotides or with a limited number of ssDNA sequences. RPA binding preferences for non-ssDNA structures have been addressed in relatively few studies. For example, hRPA binds to telomeric G-quadruplex-forming sequences and can melt a DNA triple helix (*20, 21*), and the heteromeric core of hRPA can recognize partial DNA duplexes even when the A and B domains have been deleted from hRPA70 (*22*).

From published information, it appears that the ability of hRPA to unfold G-quadruplexes depends on the nature of the G-quadruplex and the experimental conditions (*20, 21*). A 21-mer intramolecular G-quadruplex formed from a human telomeric sequence can be unfolded by hRPA in 50 mM NaCl or KCl at 20 °C, as determined by fluorescence resonance energy transfer experiments (*20*). On the other hand, hRPA was not able to dissociate intermolecular four-stranded G-quadruplexes at 25 mM KCl and 30 °C, according to EMSA data (*21*); these latter quadruplexes were formed from four strands of either a 49-mer mouse immunoglobulin switch region sequence leaving 21 nt 5′ tails or a 30-mer with two repeats of the human telomeric sequence leaving 18 nt 5′ tails.

To help resolve this inconsistency, in this study we show using EMSA and CD spectroscopy that hRPA readily forms complexes with two quadruplex structures (I-3c26 and G-8c26; see Figure 1) in a physiological buffer at 37 °C. The binding of hRPA to quadruplex-forming sequences is as facile as it is to comparable non-quadruplex-forming sequences, and the strength of hRPA binding and unfolding of a quadruplex is dependent on the thermal stability of the quadruplex.

We make use of CD spectroscopy to monitor the interaction of hRPA with these G-quadruplexes. Our recent experimental and theoretical work on the CD spectra of G-quartets (*24* and references cited therein) provides evidence that having adjacent G-quartets of both stacking polarities yields CD positive bands both at 255−260 nm (from the quartets stacked with the same polarities) and near 290 nm (from the quartets stacked with opposite polarities). The quadruplexes used in this study have one or both of these bands that allow detection of the quadruplex structural changes during hRPA binding.

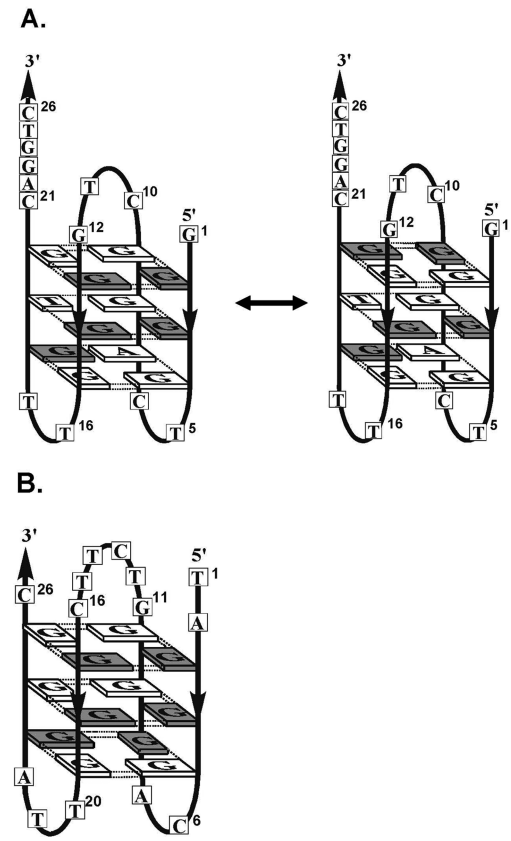

FIGURE 1: Schematics of G-quadruplexes formed by 26-mers I-3c26 and G-8c26. Bases involved in the quartets are shown as rectangles. The gray and white rectangles represent *syn* and *anti* conformations of glycosyl bonds, respectively. (A) The I-3c26 quadruplex on the left is the structure in 200 mM NaCl at 37 °C as modeled by Wen et al. (*23*). It has two neighboring quartets of the same hydrogen bonding polarity (the two at the top) and two neighboring quartets of opposite hydrogen bonding polarity (the two at the bottom). The structure on the right represents a possible quadruplex in which neighboring quartets are only of opposite hydrogen bonding polarity, consistent with CD spectra of heat-treated I-3 and I-3c26 in 200 mM KCl at 37 °C. (The 58-mer sequence I-3 has a central G-quadruplex structure like I-3c26 with additional 16 nt extensions at the 5′ and 3′ ends.) (B) G-8c26 is shown folded into a structure like that of I-3c26 in 200 mM NaCl at 37 °C, conditions under which their CD spectra are very similar. G-8c26 has a sequence that can form three adjacent quartets that contain only guanines.

EXPERIMENTAL PROCEDURES

DNA Sequences. DNA sequences I-3, I-3c26, G-8c26, and I-7 were purchased from Oligos Etc. (Wilsonville, OR); sequences I-3c26comp and RI-1 were purchased from the Midland Certified Reagent Co. (Midland, TX). The first four were derived after eight rounds of SELEX selection for binding to Ff g5p to form saturated complexes as previously described (*25*); I-7 was one of four pyrimidine-rich sequences among 36 cloned sequences that did not represent the majority of G-rich sequences selected for binding to g5p, and it is used as a control. RI-1 was selected after eight rounds of SELEX with hRPA by a procedure similar to that used with g5p, with the exception that amplification was of intermediate, and not saturated, complexes formed at low P/S (protein/DNA strand) ratios. From among 39 cloned sequences after eight rounds of SELEX, RI-1 was represented 12 times, and there were seven other very closely related sequences that had at most one change within 18 nt of the two segments of the RI-1 sequence that are underlined below. Fourteen of these nucleotides (seven from each segment) could pair to form part of an intramolecular hairpin. The SELEX-selected sequences were from a library of 58-mers with the sequence 5′-d(CGGGATCCAACGTTTT-N_{26}-AAGAGGCAGAATTCGC)-3′ in which the initial central 26 nt segment, N_{26}, was synthesized with random A, T, G, and C. The I-3 58-mer sequence contained the central G-rich sequence of 5′-d(**GGGG**TCA**GG**CT**GGGG**TT**GT**GCAGGTC)-3′. The central sequence of 26 nt by itself was I-3c26. Similarly, the 26-mer G-rich G-8c26 sequence was 5′-d(TA**GGG**CA**GGGG**TCGTC**GGG**TTA**GGG**C)-3′. I-7 was a 58-mer with the same 16-nucleotide 5′ and 3′ ends as I-3, but it had a central 26 nt pyrimidine-rich sequence of 5′-d(GTGCCACCCTCCTCTCTTGTTCTTGT)-3′. I-3c26comp was a 26-mer oligomer with a 5′-d(GACCTGCACAACCCCAGCCTGACCCC)-3′ sequence that was complemen-

tary to I-3c26. The 58-mer RI-1 sequence had a central 26 nt sequence of 5′-d(GGGGAGTTGGAGACCGCTCATTCCCC)-3′.

Concentrations of oligomers were determined by absorption measurements and extinction coefficients at 260 nm, ε_{260}, essentially the same (within 3%) as nearest-neighbor calculations for the single strands according to Gray et al. (*26*). The calculated ε_{260} values for I-3, I-3c26, G-8c26, I-7, I-3c26comp, and RI-1 were 5.74, 2.55, 2.62, 5.40, 2.36, and 5.69×10^5 M^{-1} cm^{-1} per mole of strand, respectively.

Replication Protein A. The hRPA was expressed from a pET-15b vector in *E. coli* strain BL21(DE3)pLysS (*27, 28*). The N-termini of hRPA-70 and hRPA-14 were conjugated with plasmid-encoded hexahistidine tags (MGSSHHHHHH-SSGLVPRGSHM), used for protein purification. Transformed BL21(DE3)pLysS cells were grown in 3 L of Luria broth medium supplemented with 100 μg/mL ampicillin, at 37 °C, overnight without shaking. Then fresh 100 μg/mL ampicillin was added to the medium, and the overnight culture was aerated by being shaken and incubated at 37 °C until the optical density at 600 nm was 0.6. At this point, 0.5 mM isopropyl β-D-thiogalactopyranoside was added to induce RPA expression, and incubation with aeration was continued for 3 h. Cells were harvested by centrifugation at 4 °C and 5200*g* for 20 min.

For protein purification, the cells were suspended in buffer A [500 mM NaCl, 20 mM sodium phosphate (pH 7.5), 5 mM imidazole, 10 μM $ZnCl_2$, 1 mM dithiothreitol, and 3% (v/v) glycerol] containing a protease inhibitor cocktail (Sigma p8849). The cells were lysed on ice via sonication for 30 s at 2.5 min intervals for six repeats. Lysates were clarified by centrifugation at 66200*g* and 4 °C for 20 min and loaded on a 5 mL Ni^{2+} HiTrap chelating column (Sigma), which was charged with 0.1 M nickel sulfate and equilibrated in buffer A. After the lysates had been loaded, the column was washed with (a) 20 column volumes of buffer A containing 0.01% (v/v) Nonidet P40 with 20 mM imidazole, (b) 9 column volumes of buffer A containing 40 mM imidazole, and (c) 10 column volumes of buffer A containing 100 mM imidazole. Finally, (d) the hRPA heterotrimer was eluted in 10 column volumes of buffer A containing 250 mM imidazole, which yielded almost pure hRPA subunits eluting together. The eluate was dialyzed overnight at 4 °C against hRPA binding buffer [200 mM KCl, 20 mM Tris-HCl (pH 7.4), 10 μM $ZnCl_2$, 1 mM dithiothreitol, and 1.5 mM $MgCl_2$] containing 3% (v/v) glycerol. Dialyzed protein samples were concentrated using a Centriprep centrifugal filter tube (Millipore) to a final concentration of 5−7 μM. To detect and quantitate fractions containing the RPA, protein samples were assayed by 12% SDS−PAGE (*29*) run in Tris-glycine buffer [25 mM Trizma base (pH 8.3), 192 mM glycine, and 0.1% (w/v) SDS], stained with Coomassie blue, and scanned with a document scanner. The purity of hRPA was determined with ImageQuant, version 5.0 (GE Healthcare), comparing the sum of the areas of the bands of the three subunits with the sum of the areas of all other bands. The purity of all RPA preparations was >95%.

The concentrations of hRPA heterotrimer preparations were determined by absorbance measurements at 280 nm in binding buffer using an extinction coefficient ε_{280} of 89085 M^{-1} cm^{-1} per mole of heterotrimer determined by the method of Pace et al. (*30*), after correction for 6−7% light scattering. Molecular masses of the three subunits of hRPA were verified to be 70 ± 4, 32 ± 1, and 15 ± 1 kDa from a comparison of the mobilities of the three subunits with those of standard molecular markers by 12% SDS−PAGE.

To demonstrate that the three subunits of hRPA associate as a heterotrimeric complex, hRPA from representative preparations was applied to a G75 Sephadex gel filtration column. Only one peak was detected from an elution with one-half column volume of hRPA binding buffer. Fractions from this peak were concentrated by ~8-fold to a final concentration of 6.6 μM and analyzed via 12% SDS−PAGE. The three subunits of hRPA coeluted in the same proportions as in the applied sample, confirming that the three subunits of hRPA were associated as a heterotrimer when applied to the column. In further experiments, Western blotting showed that all three subunits of hRPA were bound to the RI-1 oligomer to form complexes with discrete mobilities.

Electrophoretic Mobility Shift Assay (EMSA). An EMSA was used to identify different hRPA−DNA complexes. The protocol was as follows. (a) ssDNA was labeled with [γ-^{32}P]ATP (MP Biomedicals) at the 5′ terminus using T4 polynucleotide kinase (New England BioLabs). To remove secondary structure, the ^{32}P-labeled ssDNAs were heated at 95 °C for 3 min and cooled at 4 °C for 10 min. Then, the ^{32}P-labeled ssDNA (1 μM) was incubated with increasing concentrations of hRPA (from 0 to 6 μM) for 15 min at either RT (room temperature of 23 ± 2 °C) or 37 °C, in hRPA binding buffer. The stock protein solution also contained 3% (v/v) glycerol. (b) The hRPA−ssDNA mixture was electrophoresed on a 6% native polyacrylamide gel in 0.5× TBE buffer [90 mM Tris-HCl (pH 7.4), 20 mM boric acid, and 2 mM EDTA] at 150 V for 2 h. (c) Gels were fixed in 50% methanol and 10% acetic acid and dried at 80 °C for 1 h. Dried gels were exposed to a storage phosphor screen. The radioactive bands were visualized by autoradiography with a STORM 840 scanner (GE Healthcare) with excitation at 635 nm (red light). Data were quantitated with ImageQuant, version 5.0.

Western Blotting. Western blotting of hRPA was carried out from 6% native polyacrylamide gels such as that used for the EMSA. The gel image was transferred to a polyvinylidene fluoride (PVDF) membrane (Millipore Immobion-P), which was immersed in TBST buffer [50 mM Tris-HCl (pH 7.4), 100 mM NaCl, and 0.05% (v/v) Tween 20] with 5% (v/v) skim milk for 1 h and then incubated for 60 min at room temperature with one of the following primary antibodies each diluted 1:1000 in the same buffer: mouse monoclonal anti-RPA70 (CalBiochem NA13), goat polyclonal anti-RPA32 (Santa Cruz Biotechnology SC-14692), or mouse monoclonal anti-RPA14 (GeneTex GTX70240). After incubation with primary antibodies, the PVDF membranes were washed in TBST buffer, 10 min for three repeats. Next, the PVDF membranes were incubated with secondary antibodies of alkaline phosphatase-conjugated goat anti-mouse monoclonal antibody (Jackson ImmunoResearch) for anti-RPA14 and anti-RPA70 and alkaline phosphatase-conjugated rabbit anti-goat polyclonal antibody (Jackson ImmunoResearch) for anti-RPA32, each diluted 1:5000 in TBST buffer with 5% (v/v) skim milk for 1 h at room temperature. After incubation with secondary antibodies, the PVDF membranes were washed with TBST buffer, 10 min for three repeats.

The hRPA proteins were detected with ECF (enhanced

chemifluorescent) substrate (Amersham) and were visualized with a STORM 840 scanner (GE Healthcare) with excitation at 450 nm (blue light).

Spectral Measurements. A Jasco (Easton, MD) model V-650 spectrophotometer was used for measuring the absorption spectra of protein and oligomers at 20 °C and determination of stock concentrations. CD spectra were recorded using a Jasco model J715 spectropolarimeter. CD spectral data of the hRPA protein in binding buffer (with 3% glycerol) and of DNA oligomers in binding buffer without dithiothreitol or glycerol were acquired as the averages of six accumulations with spectral band widths of 1−2 nm. Spectra were exported at 1 nm intervals from the Jasco Spectra Manager program, smoothed by iterations of a Savitzky−Golay 13-point quadratic-cubic function (*31*), and plotted at 1 nm intervals as molar CD ($\varepsilon_L - \varepsilon_R$), in units of M^{-1} cm^{-1} per mole of amino acid residue or per mole of nucleotide.

CD spectra of hRPA were recorded in a 1 mm cuvette at 20, 30, or 37 °C over the wavelength range from 320 to 190 nm. CD spectra of three independent hRPA preparations at 20 °C were averaged and analyzed for secondary structure content using the CDPro software package (*32, 33*) at 1 nm intervals from 240 to 200 nm in units of M^{-1} cm^{-1} per mole of residue. Three methods of analysis in CDPro, CCSTR, CONTILL, and SELCON3, were used with a reference set of 48 proteins to estimate the secondary structure content of the hRPA heterotrimer.

Temperature-dependent CD spectra of oligomers were recorded in a 1 cm cuvette at increasing temperatures from 20 to 80 °C at 10 °C temperature intervals, with a 10 min incubation time before each spectrum. For CD titrations of DNA with hRPA, oligomers were in binding buffer (at a strand concentration of 0.9−2.5 μM) and were titrated with hRPA (at a concentration of 4.5−9 μM) up to P/S molar ratios of 4 in binding buffer with 3% glycerol at either 20 or 37 °C. Samples were incubated for 10 min before each spectrum was recorded after being gently mixed with the protein.

UV Melting. UV melting profiles of oligonucleotides were obtained at 260 nm using a model UV-2401 PC spectrophotometer (Shimadzu) and the Shimadzu melting temperature (T_m) analysis program 1.0.0.7 (Shimadzu). Samples were melted from 15 to 95 °C at 1 °C temperature intervals, with a 1 min incubation time before the acquisition of each point. The T_m was defined as the local maximum of the first derivative of the melting profile.

Stoichiometry Measurements. To determine the stoichiometry of complexes between hRPA and the RI-1 oligomer, EMSA experiments were used to measure the amount of DNA and Western blotting was used to determine the amount of hRPA 70 kDa subunit in a complex. Known amounts of the hRPA and ^{32}P-labeled RI-1 oligomer were included in the same gel as standards. Protein−oligomer mixtures and standards were electrophoresed on a 6% native mini-PAGE in 0.5× TBE buffer, at 150 V, for 1 h.

The concentrations of RI-1 in hRPA−RI-1 complexes were determined as in other EMSA experiments. To determine the concentrations of hRPA in the complexes, the same gels after autoradiography were used for Western blotting as described above.

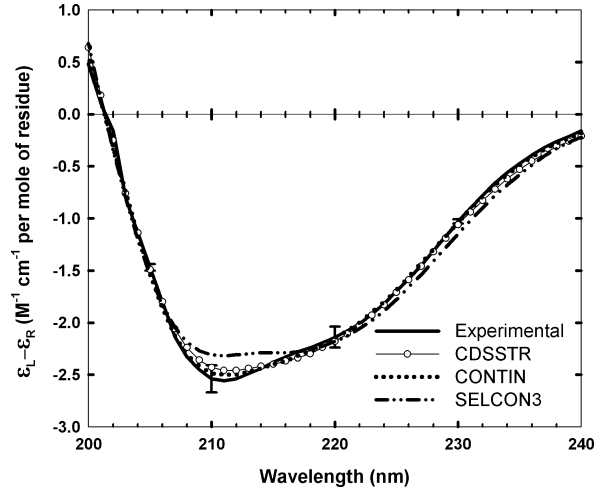

FIGURE 2: CD spectrum of hRPA at 20 °C fit by three secondary structure analysis programs. The experimental spectrum of RPA (—) was fit by secondary structure analysis programs CDSSTR (○), CONTIN (•••), and SELCON3 (−••−). The experimental CD spectrum was the average of spectra of three independent hRPA preparations, and error bars are standard deviations. The concentration of RPA was ~5 μM, and the buffer was binding buffer [200 mM KCl, 20 mM Tris-HCl (pH 7.4), 10 μM $ZnCl_2$, 1 mM DTT, and 1.5 mM $MgCl_2$] with 3% (v/v) glycerol. Spectra are plotted as $\varepsilon_L - \varepsilon_R$ in units of M^{-1} cm^{-1} per mole of residue.

Table 1: Percentages of hRPA Secondary Structures from CD Analyses[a] and from DSSP[b] Analyses of Available Crystallographic Structures

	helix (%)[c]	β-sheet (%)[d]	β-turn (%)	unordered (%)	total (%)
CD analyses	18.3 ± 0.5	28.1 ± 0.5	21.1 ± 0.2	31.2 ± 2.1	98.7 ± 1.7
DSSP	14.7	30.4	7.05		

[a] CD percentages were the averages and standard deviations from three analysis programs, CONTIN, SELCON3, and CDSSTR, of the average spectrum of three independent measurements. CD spectra were recorded in binding buffer [200 mM KCl, 20 mM Tris-HCl (pH 7.4), 10 μM $ZnCl_2$, 1 mM DTT, and 1.5 mM $MgCl_2$] with 3% (v/v) glycerol. Spectra recorded from 240 to 200 nm were analyzed with a reference set of 48 proteins. [b] A total of 77% of the hRPA amino acid residues have been crystallized, and the DSSP analyses (*34*) of these were added. Protein Data Bank entries 1fgu (*35*), 1l1o (*36*), and 2b29 (*37*). [c] Helical structure included α and distorted helix. [d] β structure included regular and distorted β-sheet.

RESULTS

CD Spectrum of hRPA. Protein CD spectra at ultraviolet wavelengths shorter than ~250 nm are dominated by peptide secondary structures. The experimental CD spectrum of hRPA at short wavelengths is shown in Figure 2. The spectra were recorded at 20 °C with the protein in binding buffer and 3% (v/v) glycerol. Negative bands of α-helical structures occur typically at 208 and 222 nm, and the bands observed for hRPA at ~210 and ~220 nm are indicative of some helical content. CD spectral analyses with CDSSTR, CONTIN, and SELCON3 (*32, 33*) gave 18.3 ± 0.5% helical structure and 28.1 ± 0.5% β-sheet, percentages that correlate reasonably well with the secondary structures that have been determined so far for 77% of hRPA residues by crystallography (Table 1 and footnotes). Figure 2 also shows spectral fits calculated with these three programs. Two of the three calculated spectra were within the measurement error.

Since our binding experiments were usually conducted at 37 °C, CD spectra of hRPA were compared at 20, 30, and

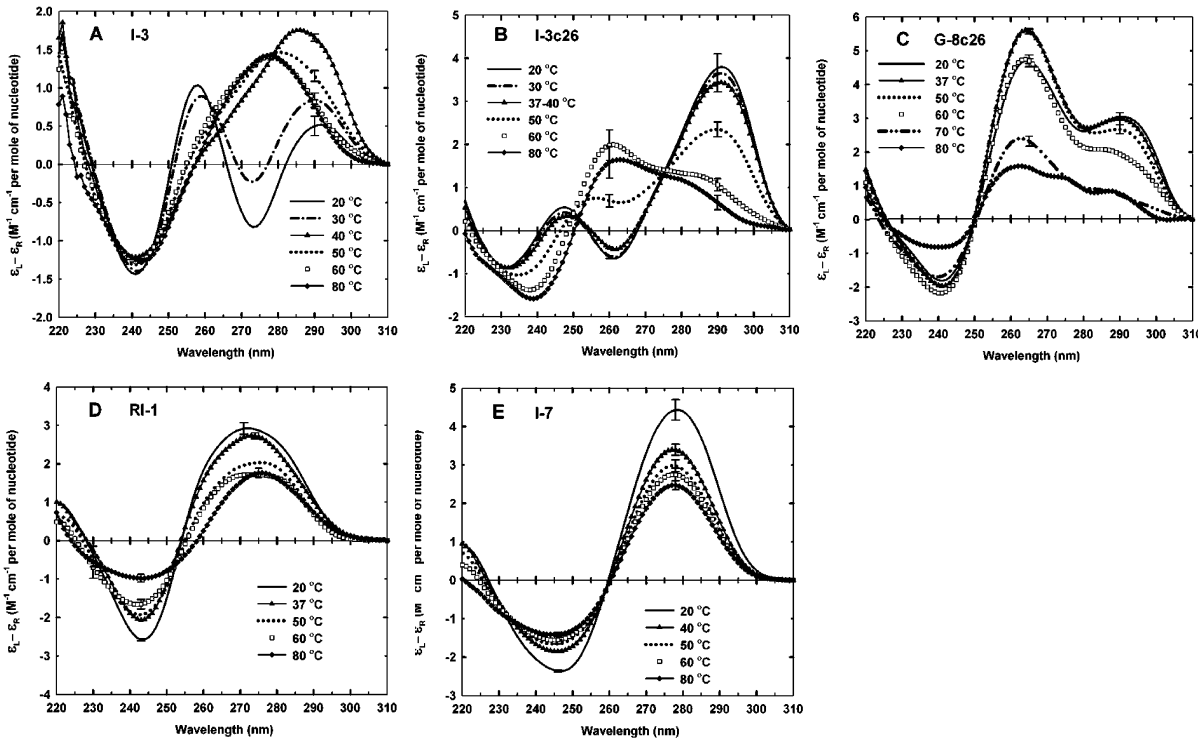

FIGURE 3: CD spectra of DNA oligomers as a function of temperature. The oligomers were (A) I-3, (B) I-3c26, (C) G-8c26, (D) RI-1, and (E) I-7. Spectra are shown at five or six representative temperatures: 20 (—), 30 (—•—), 37 or 40 (▲), 50 (•••), 60 (□), 70 (—••—), and 80 °C (◆). The buffer was binding buffer without DTT [200 mM KCl, 20 mM Tris-HCl (pH 7.4), 10 μM $ZnCl_2$, and 1.5 mM $MgCl_2$]. Spectra are plotted as $\varepsilon_L - \varepsilon_R$ in units of M^{-1} cm^{-1} per mole of nucleotide. Error bars are the ranges of duplicate measurements.

37 °C and found to be essentially identical (Figure S1 of the Supporting Information). Thus, the secondary structure of hRPA did not detectably change from 20 to 37 °C. However, the protein irreversibly precipitated upon being heated to 50 °C. Under the measurement conditions in this work, the CD of hRPA at wavelengths longer than 250−260 nm was <1% of the magnitude at 210 nm at all temperatures.

A decrease in negative CD band magnitudes has been used to monitor the denaturation of hRPA by urea (*38*), but CD measurements have not been routinely used to characterize or study hRPA. Wyka et al. (*39*) presented a CD spectrum of hRPA at 25 °C and 100 mM KCl that has a negative band at 222−224 nm, very close to the same magnitude of the negative band we measured at ∼220 nm. However, their spectrum approached zero near 210 nm with no evidence of a second negative band. The CD spectrum measured by Nuss and Alter (supplementary data in ref *38*) for hRPA at 20 °C in a low-salt buffer did have a negative peak at 210−211 nm and a broad shoulder in the vicinity of 220 nm, with roughly one-half the magnitude of the spectrum shown in Figure 2. From the few measurements to date, it appears that the CD spectrum of hRPA is sensitive to the exact preparation of the heterotrimer and the measurement conditions.

CD Spectra of DNAs. Quadruplex sequences chosen for this work were previously identified via the SELEX method (*40, 41*) as favorable aptamers for the prokaryotic Ff g5p SSB (*23, 25*). g5p is a stable dimer with each protein monomer having an OB-fold DNA-binding domain homologous to the A and B domains in hRPA. Moreover, the g5p and domains of hRPA introduce similar CD perturbations into single-stranded nucleic acids (*42*). Quadruplex sequences were selected from an in vitro library of 58-mers having a central random segment of 26 nt and flanking 16-mer primer binding sites. The two most predominant sequences, named I-3 and G-8, that were selected from this library for binding to g5p were G-rich, and by the use of CD spectroscopy, chemical modification, and other experiments, the G-rich 26-mer segment of I-3 (I-3c26) was determined to fold into an intramolecular G-quadruplex of three potential G-quartets in 200 mM NaCl, two of which were proposed to have a non-guanine base, as shown in Figure 1A (left) (*23*). The first and second G-quartets (the two closest to the 3′ and 5′ ends) are stacked with the same hydrogen binding polarities, and the second and third G-quartets are stacked with opposite polarities, consistent with its CD spectrum (*24, 43*) in 200 mM NaCl. On the basis of its CD spectrum, the related G-8c26 sequence is assumed to have a similar structure in 200 mM NaCl (*23*) (see Figure 1).

CD spectra are particularly useful in investigating the binding of proteins to a nucleic acid when the nucleic acid has distinct CD bands in the ultraviolet region above 250 nm, where proteins have relatively small CD bands due only to the optical activity of aromatic amino acids (*44*). Intramolecular DNA G-quadruplexes such as I-3, I-3c26, and G-8c26 that have G-quartets stacked with opposing hydrogen bonding polarities have CD spectra characterized by a positive CD band near 290 nm (*24, 43*). The presence of this CD band is diagnostic of the presence of the quadruplex structure. Thus, the perturbation or disruption of these quadruplexes by heating or by forming complexes with hRPA can be readily detected by CD spectroscopy.

Figure 3 summarizes the temperature dependence of each of the CD spectra of oligomers used in this study. The spectrum of I-3 at 20 °C in the presence of 200 mM KCl (Figure 3A) had two positive bands at ∼260 and ∼290 nm,

Table 2: Absorbance Melting Temperatures (T_m) and Percent Hyperchromicities (*%H*) of the Dominant Transitions in the Melting Profiles of I-3, I-3c26, G-8c26, RI-1, and I-7 at 200 mM KCl[a]

oligomer	T_m (°C)[b]	*%H*[c]
I-3[d]	39.4 ± 0.6	7.7 ± 1.3
I-3c26	55.0 ± 0.4	4.5 ± 0.1
G-8c26	68.0 ± 0.3	7.7 ± 0.2
RI-1	71.0 ± 1.0	7.6 ± 0.6
I-7[e]	34.9 ± 0.9	10.7 ± 0.7

[a] Values for all but I-7 are averages and ranges from two independent measurements in binding buffer [200 mM KCl, 20 mM Tris-HCl (pH 7.4), 10 μM $ZnCl_2$, and 1.5 mM $MgCl_2$, but without DTT, except for one of two measurements for RI-1 which was carried out in the presence of 1 mM DTT] or 200 mM KCl and 10 mM Tris-HCl (pH 7.4). The absorbance was monitored at 260 nm except that for G-8c26, which was monitored at 256 nm. [b] T_m values are from derivatives of the melting profiles. [c] *%H* values are the percent increases in absorbance from the beginning to the end of the cooperative transition. [d] From CD spectra, the G-quadruplex segment of I-3 melts at 40−60 °C, in agreement with the T_m for I-3c26, but this transition was not detected in the melting profile. [e] Values are the averages and ranges from one determination in binding buffer and one in 200 mM NaCl and 10 mM Tris-HCl (pH 7.4).

essentially identical to the spectrum previously published for this 58-mer at 5 °C in the presence of 200 mM NaCl (*23*). These two bands resulted from the quadruplex structure of the 26 nt core (Figure 1A, left). There were two transitions in the I-3 structure as the temperature increased. First, the longer-wavelength positive band increased in magnitude as the temperature increased to 40 °C, and the 260 nm band was lost. This was consistent with a shift to a quadruplex dominated by an alternating polarity of neighboring G-quartets (Figure 1A, right), combined with the loss of extraneous base pairing involving the 16-mer tails of the I-3 sequence as ascertained in previous work (*23*). This first transition had a T_m of ~39 °C in absorbance melting profiles (Table 2). Second, the positive CD band at 285−290 nm was lost as the temperature was increased from 40 to 60 °C, indicative of disruption of the core quadruplex. This second transition was not detected in absorbance melting profiles in the presence of 200 mM KCl, and it was difficult to detect in the presence of 200 mM NaCl (*23*). However, it was confirmed by CD spectra and melting profiles of just the central 26-mer quadruplex-forming sequence, I-3c26, in 200 mM KCl (Figure 3B and Table 2).

CD spectra of I-3c26 with K^+ ion at 20 and 37 °C were dominated by the 290 nm positive band (Figure 3B), whereas spectra of I-3c26 with Na^+ ion at these temperatures had two positive bands of similar magnitude at 250−260 nm and at 290 nm (*23, 24*). We interpret this ion-dependent spectral difference as signifying a shift in the preferred polarity of stacked quartets, with neighboring quartets of opposite polarities being favored in the presence of K^+ (as in Figure 1A, right). In any case, CD spectra showed that I-3 and I-3c26 retain quadruplex structures at 37 °C in binding buffer.

The G-8c26 oligomer sequence is also able to form a quadruplex, presumably analogous to that of the I-3c26 quadruplex but with three stacked quartets containing only guanine bases. In the case of G-8c26 in the presence of K^+ ion, there was a CD band at ~265 nm (Figure 3C) that was larger than the 290 nm band, indicative of an enhanced interaction of G-quartets stacked with the same polarity. A band at 290 nm in the spectrum of G-8c26 at 20 and 37 °C was evidence that this sequence, like I-3c26, had at least one pair of neighboring quartets that was stacked with opposite polarities. The G-8c26 quadruplex was more thermostable than the I-3c26 quadruplex in the presence of either 200 mM Na^+ or 200 mM K^+ [Table 2 (*23*)].

While the I-3 and G-8 quadruplex-forming sequences were originally selected as binding sites for the prokaryotic OB-fold gene 5 protein, RI-1 was selected for binding to hRPA by a similar SELEX procedure (see Experimental Procedures). The CD spectrum of RI-1 (Figure 3D) did not exhibit a band near 260 or 290 nm that would indicate the formation of a G-quadruplex. The magnitudes of its CD bands generally decreased as a function of temperature, as expected for a decreased level of base−base stacking, but there was also a minor change in spectral shape in the 255−275 nm region as the temperature increased from 60 to 80 °C. This CD transition was consistent with the T_m of 71.0 ± 1.0 °C detected in absorbance melting profiles at 260 nm (Table 2). Portions of this sequence (underlined in Experimental Procedures) could be involved in a base-paired stem and loop structure with 10 contiguous base pairs [at 37 °C and 1 M NaCl; *RNAstructure*, version 4.6 (*45*)]. Thus, the CD spectra of RI-1 were consistent with the existence of a segment of normal Watson−Crick base pairs at 37 °C, but not with the presence of a G-quadruplex structure.

A pyrimidine-rich I-7 sequence, for which the g5p has less affinity than for I-3 (*23*), was used as a control. It had no extensive secondary structure as indicated by its classical conservative CD spectrum in which there is a positive band above and a negative band below a crossover near 260 nm, and by the simple decrease in the magnitudes of these CD bands with an increase in temperature [Figure 3E (*46*)]. There was a detectable T_m at 34.9 ± 0.9 °C in absorbance melting profiles, but this probably involved melting of a relatively few base pairs. The longest stretch of contiguous base pairs predicted by the *RNAstructure* program was four. Whatever base pairing may exist in I-7 at lower temperatures, our spectral data show that this DNA is essentially unstructured at 37 °C.

The CD spectrum of I-3c26comp (not shown) also exhibited the conservative CD spectral shape expected for a ssDNA having no unusual secondary structure, and no base pairing was predicted by *RNAstructure*.

EMSA and CD Spectra Show That hRPA Binds and Melts Quadruplex DNAs. Gel mobility shift experiments and CD titrations with hRPA were generally performed at 37 °C in a binding buffer that approximated a physiological environment, while including Zn^{2+} ion and DTT as required to stabilize the protein (*47*). EMSA data for each of the DNA sequences described above upon titration with hRPA are shown in Figure 4. The DNAs were ^{32}P-labeled at the 5′ ends, mixed with hRPA at increasing protein/strand (P/S) ratios at either RT or 37 °C, run on 6% native polyacrylamide gels, and assayed as described in Experimental Procedures. The DNAs were kept at a constant concentration close to 1 μM, so that at a P/S ratio of 1.0 the hRPA concentration was also 1 μM and there was nominally one hRPA heterotrimer present per 58-mer or 26-mer strand of DNA. The effective P/S ratios varied by as much as ±30%, as estimated from the reproducibility of repeat measurements with different hRPA preparations. However, it was clear that hRPA−DNA complexes with discrete mobility shifts were formed upon addition of hRPA to all of the DNAs (Figure

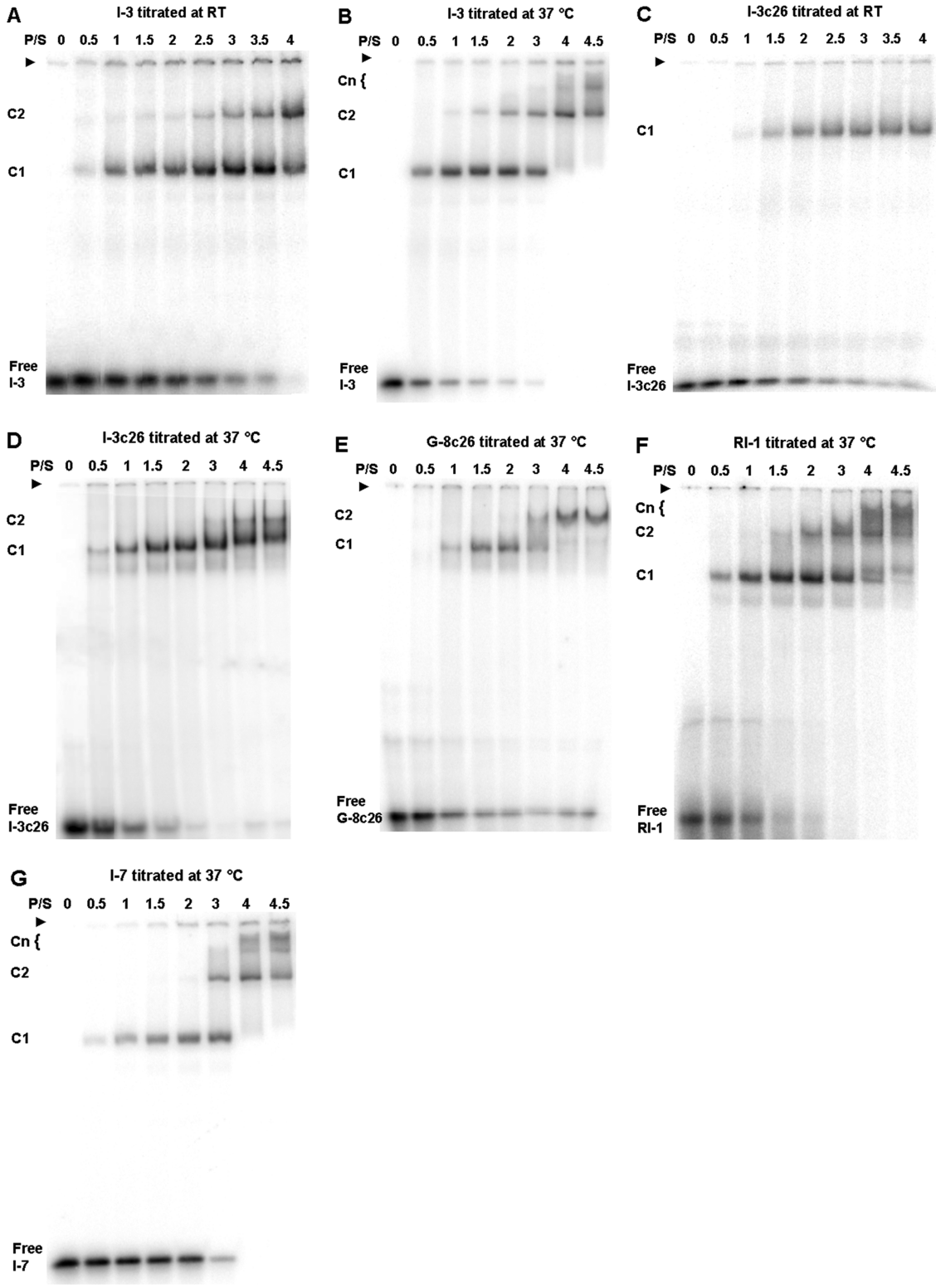

FIGURE 4: Representative EMSA results. ^{32}P-labeled DNA oligomers were titrated with hRPA at the P/S (protein/oligomer strand) ratios indicated at the tops of the lanes, run on 6% native polyacrylamide gels, and autoradiographed. (Not all lanes are shown for each gel, but data at all P/S ratios are included in the binding profiles in Figure S2 of the Supporting Information.) The oligomers were (A) I-3 at RT, (B) I-3 at 37 °C, (C) I-3c26 at RT, (D) I-3c26 at 37 °C, (E) G-8c26 at 37 °C, (F) RI-1 at 37 °C, and (G) I-7 at 37 °C. C1 denotes the complex of highest mobility, C2 a complex with approximately one-half the mobility of C1, and Cn still lower-mobility complexes that can form with the 58-mer oligomers at 37 °C. The buffer was hRPA binding buffer [200 mM KCl, 20 mM Tris-HCl (pH 7.4), 10 μM $ZnCl_2$, 1 mM DTT, and 1.5 mM $MgCl_2$].

4). The complexes were denoted as C1 (the complex formed at the lowest P/S ratios) and C2 (the complex having approximately one-half of the mobility of C1 and formed at higher P/S ratios). Cn denotes the spread of complexes of still lower mobilities at the highest P/S ratios.

Western blots in Figure 5 demonstrated that the C1 and C2 complexes with RI-1 each contained all three of the hRPA subunits. Similar data were obtained with other 58-mer sequences (not shown). The relative amounts of each of the hRPA subunits (from the intensities of the Western blots)

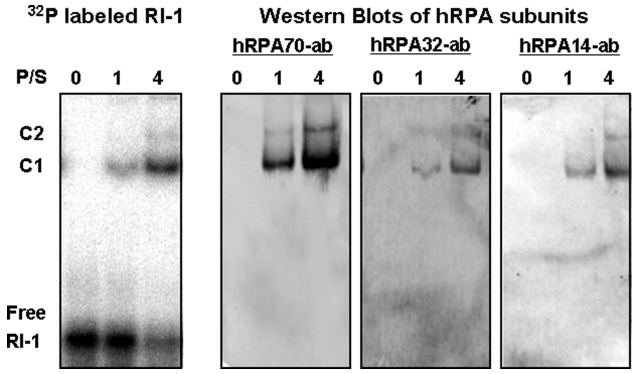

FIGURE 5: Western blots identified three subunits of hRPA present in the C1 and C2 complexes. A 6% native polyacrylamide gel showing the C1 and C2 bands of ^{32}P-labeled RI-1 with hRPA at P/S ratios of 1 and 4 was autoradiographed (three left-hand lanes). Then the bands were transferred to a membrane and used for Western blotting with the antibody (ab) to one of the three subunits of hRPA. Three parallel Western blot experiments showed that all three hRPA subunits were present (nine right-hand lanes) in both the C1 and C2 complexes. The relative intensities of hRPA subunits in the C2 and C1 complexes, compared with the relative intensities of the DNA present, yielded the ratios of protein present in the two types of complex.

in the two types of complexes were in the ratio of 2.3 ± 0.4 (Table 3, first row). In addition, the amounts of ^{32}P-labeled DNA and hRPA70 subunit (from separate experiments similar to those depicted in Figure 5) in the C1 and C2 complexes were quantitated to give hRPA/DNA ratios of 1.3 ± 0.3 for C1 and 2.0 ± 0.01 for C2 (Table 3, second row). The quantitation was based on standard curves of known concentrations of free DNA and free hRPA that were run on the same gel. The simplest explanation of the results listed in Table 3 is that the complexes labeled as C1 and C2 were formed by binding one and two hRPA heterotrimers, respectively, to one strand of DNA oligomer. We assume this to be the case for all of the DNAs in this study.

The hRPA can bind to ssDNA in multiple binding modes, with 23−27 nt being required to bind all four domains (A−D) of hRPA (*9, 10*). A 58-mer oligomer could therefore accommodate two hRPA heterotrimers in the bands labeled as C2. Additional bands of lower mobility are seen in the EMSA gels for 58-mers I-3, RI-1, and I-7 at 37 °C (bands marked as Cn in panels B, F, and G of Figure 4, respectively). The existence of these bands indicated that only two (A and B) or three (A, B, and C) domains were needed to bind at P/S ratios of >4. The fact that complexes of two mobilities (C1 and C2) were observed with the 26-mers at 37 °C (Figure 4D,E) also indicated that only two or three domains were effective in binding to sites of fewer than 23−27 nt under our conditions. C2 complexes of hRPA with short 21-mer DNAs have previously been observed by others (*20*).

Our EMSA experiments were performed without protein−DNA cross-linking. Bands of complexes were nevertheless generally discrete and constant in mobility, the most obvious exception being the decreased mobility of the C1 complex formed with I-3c26 at P/S ratios greater than 2 at 37 °C (Figure 4D). This likely was a mixture of the C1 and C2 complexes, consistent with the results of Salas et al. (*20*). We also occasionally observed a faint band of greater mobility than C1 (Figure 4D−F) which remains unidentified, but this was always less than 10% of the C1 band.

The EMSA data of Figure 4 show that hRPA binds to I-3 and I-3c26 more strongly at 37 °C than at room temperature (RT). That is, there was less remaining free DNA and a greater fraction of the C1 complex at lower P/S ratios when the hRPA−DNA mixtures were kept at 37 °C rather than at RT (compare panels B and D with panels A and C, respectively, in Figure 4). Although 37 °C is below the melting temperatures of all three of the quadruplexes (I-3, I-3c26, and G-8c26), more than 60% of each of these DNAs was complexed with hRPA at P/S ratios of 1−2 at this temperature. (Binding profiles from multiple EMSA data are shown in Figure S2 of the Supporting Information).

By monitoring the CD spectra of the DNAs during titrations of the 26-mer quadruplex DNAs at 20 and 37 °C, at DNA concentrations comparable to those in the EMSA titrations, we found that the 290 nm band of I-3c26, and both long-wavelength CD bands of G-8c26, were lost as the P/S ratio increased to ∼2; see Figure 6C−E. Combined with the EMSA data of Figure 4C−E showing that the C1 complexes predominated up to this P/S ratio, the CD changes showed that one hRPA heterotrimer was apparently sufficient to stably bind to unfolded forms of these G-quadruplexes. However, we would not have detected transient complexes that occur in the initial stages of binding, such as might be detected by glutaraldedyde cross-linking (*11*).

In addition, a comparison of the CD titrations of I-3c26 at 20 and 37 °C (Figure 6C,D) supported the evidence from EMSA titrations that hRPA binding to the quadruplex structure was enhanced when the titrations were performed at the higher temperature. That is, the 290 nm CD band was lost at lower P/S ratios when the titration was performed at a temperature (37 °C) closer to the melting temperature of the quadruplex.

The CD titration of 58-mer I-3 at 37 °C resulted in a noticeable loss of the quadruplex 290 nm band (Figure 6B) at P/S ratios of up to 2, in agreement with the conclusion that the binding of hRPA can melt a quadruplex, even though in this case the quadruplex is embedded within a longer sequence. During titrations of I-3 with hRPA at 20 °C, there was a perturbation of the 260 nm quadruplex band, which is present at this lower temperature (compare Figures 3A and 6A). However, the complete loss of the I-3 quadruplex structure when titrated at 20 °C seems doubtful in that the spectrum of I-3 at the highest P/S ratios differs from that when I-3 is titrated at 37 °C or when melted to high temperatures. Specifically, the long-wavelength band in Figure 6A is not increased in magnitude, and the crossover wavelength remains above 270 nm. Thus, except possibly for I-3 at 20 °C, the binding of hRPA was concurrent with the disruption of the I-3, I-3c26, and G-8c26 quadruplex structures.

(The possibility that the long-wavelength CD spectra of the hRPA−DNA complexes in Figure 6 are significantly influenced by alterations in the protein seems unlikely given that the spectral changes are specific to the CD bands of the nucleic acids. However, at the shorter wavelengths in Figure 6, the protein contributes a modest negative CD. For example, at 250 nm, the protein contribution at a P/S ratio of 1.0 would be approximately −0.2 and −0.45 M^{-1} cm^{-1} on the per nucleotide scales shown in titrations of the 58-

Table 3: C2 Protein/C1 Protein and hRPA/DNA Ratios in C1 and C2 Complexes between hRPA and RI-1 Oligomer

experiment	C2 protein/C1 protein ratio (per equal amount of DNA)	hRPA/DNA ratio of C1	hRPA/DNA ratio of C2
Western blots	2.3 ± 0.4[a]	not available	not available
Western blots plus standard curves	2.0 ± 0.03[c]	1.3 ± 0.3[b]	2.0 ± 0.01[c]

[a] The ratio determined as (protein in C2)/(protein in C1) × (^{32}P-labeled DNA in C1)/(^{32}P-labeled DNA in C2) averaged for Western blots for all three subunits ± the standard deviation, formed at a P/S ratio of 4. [b] The average and range for C1 complexes at P/S ratios of 1 and 4 with RI-1. [c] Ratios and ranges from data on two 58-mer sequences, including RI-1, at a P/S ratio of 4.

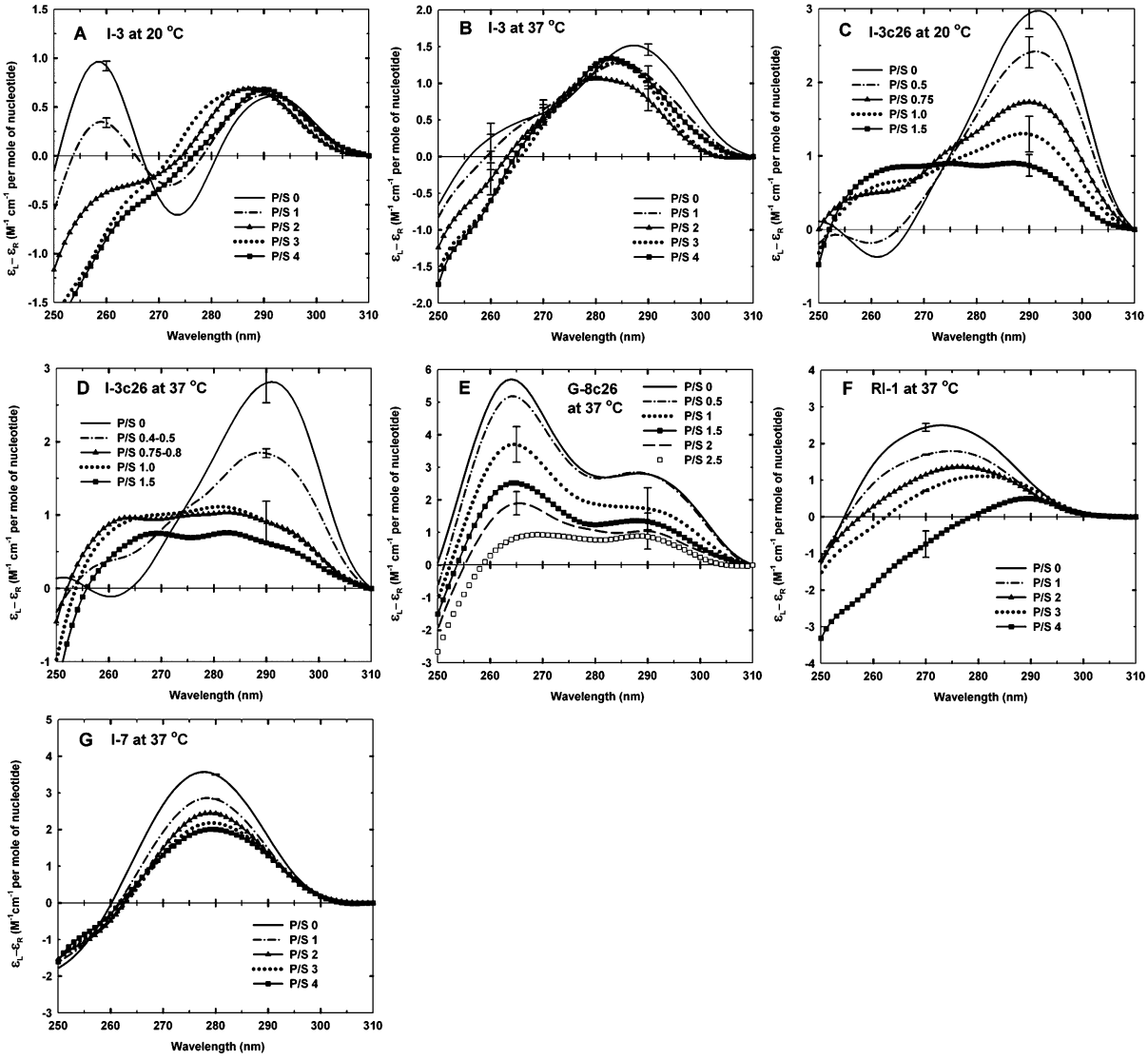

FIGURE 6: CD spectra of DNA oligomers titrated with hRPA: (A) I-3 at 20 °C, (B) I-3 at 37 °C, (C) I-3c26 at 20 °C, (D) I-3c26 at 37 °C, (E) G-8c26 at 37 °C, (F) RI-1 at 37 °C, and (G) I-7 at 37 °C. For the 58-mer sequences in panels A, B, F, and G, spectra are shown at P/S (protein/oligomer strand) ratios of 0 (—), 1 (—•—), 2 (▲), 3 (•••), and 4 (■). For the 26-mer sequences in panels C−E, spectra are shown at representative P/S ratios of 0 (—), 0.4−0.5 (—•—), 0.75−0.8 (▲), 1.0 (•••), 1.5 (■), 2.0 (– – –), and 2.5 (□). Note that the spectra of panel A are on a more sensitive molar CD scale than those of panel B. The buffer was binding buffer [200 mM KCl, 20 mM Tris-HCl (pH 7.4), 10 μM $ZnCl_2$, 1 mM DTT, and 1.5 mM $MgCl_2$]. Spectra are plotted as $\varepsilon_L - \varepsilon_R$ in units of M^{-1} cm^{-1} per mole of nucleotide. Error bars are the ranges of duplicate measurements.

mers and 26-mers, respectively. At 260 nm, the respective CD contributions would be approximately −0.07 and −0.15 M^{-1} cm^{-1}).

EMSA results with the RI-1 sequence (Figure 4F), which was selected in SELEX experiments with hRPA, resembled those for the I-3 58-mer at 37 °C (Figure 4B) and show that hRPA binds to the RI-1 58-mer with an affinity that is no greater than for the quadruplex-forming I-3. CD titrations of RI-1 (Figure 6F) were typical of those for binding of the hRPA70A domain and the prokaryotic g5p to most ssDNA oligomer sequences in that the positive long-wavelength band was reduced in magnitude while the crossover wavelength was shifted to longer wavelengths [e.g., from ~260 to ~280 nm (*42, 46*)]. This type of ssDNA CD perturbation is probably a combination of several effects, including a reduction in the number of base−base stacking interactions and an effect of nucleotide dehydration (*44*). There was no CD evidence for the disruption of a G-quadruplex or other significant secondary structure during the titration of RI-1.

Table 4: Estimates from EMSA Titrations of hRPA Apparent Binding Affinities (K_a) for Formation of C1 Complexes of One hRPA per Oligonucleotide with Various Oligonucleotide Sequences[a]

oligomer	$K_a \times 10^{-6}$ (M^{-1})	oligomer	$K_a \times 10^{-6}$ (M^{-1})
I-3 (58-mer, RT)	0.7 ± 0.1[b]	G-8c26 (26-mer, 37 °C)	2.0±0.6
I-3 (58-mer, 37 °C)	>10	RI-1 (58-mer, 37 °C)	2.0±0.6
I-3c26 (26-mer, RT)	0.8 ± 0.2	I-7 (58-mer, 37 °C)	0.7±0.1
I-3c26 (26-mer, 37 °C)	>2		

[a] Titrations were conducted in binding buffer [200 mM KCl, 20 mM Tris-HCl (pH 7.4), 10 μM $ZnCl_2$, 1 mM DTT, and 1.5 mM $MgCl_2$] at the indicated temperatures. [b] Errors are the ranges of two or more determinations.

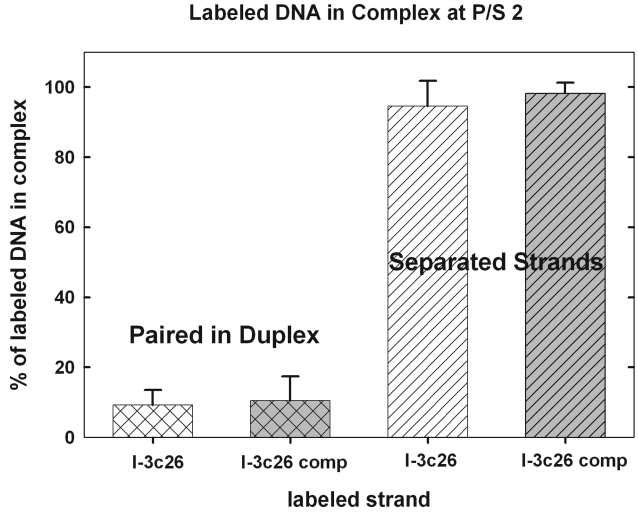

FIGURE 7: EMSA results of I-3c26 and the complementary I-3c26comp when paired as a duplex or when separated. The oligomers were labeled with ^{32}P one at a time and either mixed in a 1:1 ratio to form a duplex or treated as separate strands. The hRPA was added at a P/S ratio of 2 with respect to the total strand concentration (i.e., in the case of paired strands, the protein/duplex ratio was 4). When the oligomer was paired with its complementary strand, the percentage of label in C1 or C2 complexes was only 9−11%, compared with 94−98% of the label in complexes formed with the separated strands. Error bars are standard deviations from three to four experiments for duplexes and five to eight experiments for the separated strands.

The least favorable binding among the 58-mer sequences at 37 °C was to the unstructured I-7, which displayed the lowest proportion of C1 complexes at P/S ratios of up to 2 (Figure 4B,F,G). With respect to the corresponding CD titration of I-7 (Figure 6G), the binding of hRPA resulted in only a reduction in the magnitude of the long-wavelength positive CD band, a change typically observed during heating a ssDNA (Figure 3E) and related to a reduction in the number of base−base stacking interactions.

Apparent Binding Constants. Apparent K_a values for single-site binding of hRPA to these oligomers were estimated from the EMSA profiles as 1/[free hRPA concentration] at the P/S ratios for which 50% of the DNA remained free and 50% was bound, predominantly in C1 complexes. These estimates are summarized in Table 4. The EMSA titrations were not performed over a sufficiently wide range of P/S values to provide accurate K_a values, in addition to the fact that the number of binding sites for formation of C1 complexes is unknown and may well differ for the various oligomers. Despite these caveats, it is fairly clear that the binding affinities of hRPA for I-3 and I-3c26 at RT and for I-7 at 37 °C were similar and were the weakest at $<10^6$ M^{-1}, while the affinities for RI-1 and the quadruplex-forming sequences at 37 °C were higher at $>2 \times 10^6$ M^{-1}. The binding of hRPA to the I-3 sequence at 37 °C appeared essentially stoichiometric under the conditions studied, with a K_a of $>10^7$ M^{-1}. In additional experiments with I-3 (not shown), in which a constant concentration of hRPA was titrated with increasing concentrations of I-3, the binding affinity also was $>10^7$ M^{-1} and too high to be determined.

The binding affinities estimated for binding of the first hRPA molecule (under our conditions of 0.2 M KCl and 37 °C) were much lower than the K_a values determined by others for hRPA and scRPA binding to dT_{30}; those were on the order of 10^9 M^{-1} at NaCl concentrations of 0.1−0.2 M and at 25 °C (*48, 49*). Some of the difference may be attributed to the different binding conditions or to the DNA sequences used. Oligomers we have studied may have few and possibly only one preferred site available for binding of the first hRPA molecule. As pointed out by Kumaran et al. (*49*), there are overlapping sites on a repeating sequence oligomer such as dT_n which could account for a higher binding affinity of the first scRPA molecule compared with a second. In fact, these authors showed that the binding affinity of a second scRPA molecule for a remaining single site on dT_{30} was reduced to only 0.6×10^6 M^{-1}.

DISCUSSION

Influence of Quadruplex Structures on hRPA Activity. EMSA data in Figure 4 showed that hRPA binds to nontelomeric G-quaduplexes, and CD spectroscopy demonstrated that the G-quadruplexes (I-3, I-3c26, and G-8c26) are melted by the protein at 37 °C (Figure 6). The binding affinities of RPA for I-3 and I-3c26 were higher at 37 °C than at 20 °C and appeared to be correlated with the reduced stability of the quadruplex at a higher temperature and whether the quadruplex could be unfolded by the protein.

Additional EMSA experiments were performed to address the question of how hRPA binding to a DNA duplex, and to its separated strands, might be impacted by the presence of a purine-rich strand such as I-3c26 (with 61.5% purines) that can form an intramolecular quadruplex. First, EMSA data were obtained for binding of hRPA to the complementary sequence, I-3c26comp (shown in Figure S3 of the Supporting Information). Interestingly, hRPA binding affinity (i.e., the P/S ratio for one-half saturation) was not detectably different for the I-3c26 quadruplex and I-3c26comp sequences. Although hRPA affinity can be 50-fold higher for single-stranded DNAs that are pyrimidine-rich than for single-stranded DNAs that are purine-rich (*1* and references cited therein), this preferential binding does not always hold for specific sequences or structures of the purine-rich strand. Therefore, if an intramolecular G-quadruplex of the type formed by I-3c26 forms in a separated strand during DNA replication, it would not necessarily hinder hRPA binding during DNA

replication of that strand versus the complementary strand. The effect of sequence on hRPA binding is emphasized by the fact that hRPA had the least favorable binding to I-7, which was the most pyrimidine-rich 58-mer sequence among those we studied. The pyrimidine content of its central 26 nt region was 81%, compared with 50% pyrimidine content in the selected central sequence of RI-1 and only 38% in the central I-3c26 sequence of I-3.

Second, EMSA data were obtained for binding of hRPA to the duplex formed by pairing of I-3c26 and its complementary pyrimidine-rich strand I-3c26comp (with 61.5% pyrimidines). The formation of a duplex was shown by classical mixing experiments, monitored by native polyacrylmide gels, and the duplex had a T_m above 60 °C in binding buffer without DTT (data not shown). With each strand separately labeled in EMSA experiments with the duplex and with the separated strands, hRPA titrations were performed. The resulting data are summarized in Figure 7 at P/S ratios of 2. (The P/S ratio is with respect to the total strand concentration.) There was only minor binding of the protein to the duplex (9−11%) compared with the binding to each of the separated strands (94−98%), in agreement with other results which show that hRPA has a very low affinity for dsDNA (*1*). Thus, the fact that the sequence of a DNA strand predisposes its folding into an intramolecular quadruplex may have no effect on the destabilization by hRPA of a duplex containing this sequence. Moreover, these data provide a direct comparison for binding to duplex and quadruplex secondary structures. The quadruplex structure is the more favorable for hRPA binding, suggesting that short adjacent tails or loops of bases connecting the quadruplex strands favor the initial binding and eventual melting of a quadruplex by hRPA.

Mechanism of hRPA Bnding to Quadruplex Structures. The use of CD spectroscopy in combination with the EMSA results showed that a single heterotrimer was sufficient to maintain the melted forms of the 26-mer quadruplexes, as demonstrated by the loss of characteristic quadruplex CD bands at 290 nm for both I-3c26 and G-8c26 and the 260 nm band for G-8c26 (Figure 6C−E). There was no obvious unfolding intermediate during titrations of the 26-mer quadruplexes, since corresponding EMSA data were devoid of a significant smear of structures between the free DNA and C1 complexes (Figure 4C−E) and the major CD changes corresponding to C1 complex formation were approximately two-state (Figure 6C−E). In contrast, Salas et al. (*20*), on the basis of FRET and EMSA experiments, concluded that hRPA binding and unfolding of a 21-mer telomeric quadruplex occur in a sequential fashion via two unfolded conformations. The apparent difference in mechanism may reside in the different capabilities of the techniques used or in the specific quadruplex fold or loop sequences being studied. In any case, it seems clear that hRPA has the ability to unfold a quadruplex DNA structure, possibly by initially binding to a few unpaired nucleotides.

Finally, our data hint that hRPA prefers to bind to the 58-mer I-3 sequence because of a favorable arrangement of unpaired nucleotides adjacent to the stacked G-quartets. The I-3 structure (quadruplex with tails) was the most favorable for RPA binding among the analyzed structured (RI-1) or unstructured (I-7) DNAs. At 20 °C, a decrease in the magnitude of the 260 nm CD band of the core quadruplex structure of I-3 was the main alteration of the I-3 structure caused by binding of an hRPA molecule (Figure 6A). In related work, the 260 nm CD band of I-3 has been shown to be perturbed by initial binding of Ff g5p molecules to the quadruplex core before the protein saturates the tail sequences (*23*). That is, nucleotides constrained by the I-3c26 quadruplex fold could be favored over the less structured tails for initial binding of hRPA to I-3. A comparison of EMSA results for I-3 and I-7 at 37 °C (Figure 4B,G) provides support for this notion. C2 complexes began to dominate at similar P/S ratios of ≥3 for I-3 and I-7. Although the first molecule of hRPA had a more favorable K_a for binding to I-3 by a factor of more than 10, the second molecule was almost as readily bound to I-7 as to I-3. This is consistent with the interpretation that the quadruplex structure itself is important for the formation of C1 complexes and unfolding of the quadruplex (at 37 °C), since after the quadruplex core was disrupted there no longer was preferential binding to the I-3 sequence.

Functional Significance. The biological significance of hRPA binding and its ability to unfold at least some quadruplexes remains indirect. Human promoter sequences can form quadruplex stuctures that may well be involved in transcriptional control, as reviewed by Qin and Hurley (*50*), and the existence of G-quadruplexes in cells has been shown by the use of a quadruplex-specific ligand that binds predominantly to telomeres, but also to interstitial regions of chromosomes (*51*). The ability of RPA to bind to nucleotides in single-stranded DNA is central to its numerous functions, including DNA replication (*1–4*) and telomeric maintenance (*12–14*). Therefore, the binding and unfolding of some telomeric and nontelomeric quadruplexes by hRPA, as shown by Salas (*20*) and in this work, provides a step toward appreciating how this important protein might function within the diversity of DNA sequences and structures within the human genome.

ACKNOWLEDGMENT

We are grateful to Dr. Jin-Der Wen (Department of Chemistry, University of California, Berkeley, CA) for sharing his data on the melting profiles of I-3, G-8c26, and I-7, which were included in Table 2. We are also indebted to Dr. Carla W. Gray (Department of Molecular and Cell Biology, The University of Texas at Dallas, Richardson, TX) for sharing her expertise on protein purification.

SUPPORTING INFORMATION AVAILABLE

CD spectra of hRPA at 20, 30, and 37 °C (Figure S1), binding profiles of EMSA results for the seven oligomer and temperature combinations listed in Table 4 (Figure S2), and an EMSA gel and binding profile for titrations of I-3c26comp with hRPA (Figure S3). This material is available free of charge via the Internet at http://pubs.acs.org.

REFERENCES

1. Wold, M. S. (1997) Replication protein A: A heterotrimeric, single-stranded DNA-binding protein required for eukaryotic DNA metabolism. *Annu. Rev. Biochem. 66*, 61–92.

2. Iftode, C., Daniely, Y., and Borowiec, J. A. (1999) Replication protein A (RPA): The eukaryotic SSB. *Crit. Rev. Biochem. Mol. Biol. 34*, 141–180.
3. Fanning, E., Klimovich, V., and Nager, A. R. (2006) A dynamic model for replication protein A (RPA) function in DNA processing pathways. *Nucleic Acids Res. 34*, 4126–4137.
4. Haring, S. J., Mason, A. C., Binz, S. K., and Wold, M. S. (2008) Cellular functions of human RPA1: Multiple roles of domains in replication, repair, and checkpoints. *J. Biol. Chem. 283*, 19095–19111.
5. Murzin, A. G. (1993) OB(oligonucleotide/oligosaccharide binding)-fold: Common structural and functional solution for non-homologous sequences. *EMBO J. 12*, 861–867.
6. Raghunathan, S., Kozlov, A. G., Lohman, T. M., and Waksman, G. (2000) Structure of the DNA binding domain of *E. coli* SSB bound to ssDNA. *Nat. Struct. Biol. 7*, 648–652.
7. Skinner, M. M., Zhang, H., Leschnitzer, D. H., Guan, Y., Bellamy, H., Sweet, R. M., Gray, C. W., Konings, R. N., Wang, A. H., and Terwilliger, T. C. (2004) Structure of the gene V protein of bacteriophage f1 determined by multiwavelength X-ray diffraction on the selenomethionyl protein. *Proc. Natl. Acad. Sci. U.S.A. 91*, 2071–2075.
8. Bochkareva, E., Belegu, V., Korolev, S., and Bochkarev, A. (2001) Structure of the major single-stranded DNA-binding domain of replication protein A suggests a dynamic mechanism for DNA binding. *EMBO J. 20*, 612–618.
9. Lavrik, O. I., Kolpashchikov, D. M., Weisshart, K., Nasheuer, H. P., Khodyreva, S. N., and Favre, A. (1999) RPA subunit arrangement near the 3′-end of the primer is modulated by the length of the template strand and cooperative protein interactions. *Nucleic Acids Res. 27*, 4235–4240.
10. Bastin-Shanower, S. A., and Brill, S. J. (2001) Functional analysis of the four DNA binding domains of replication protein A. The role of RPA2 in ssDNA binding. *J. Biol. Chem. 276*, 36446–36453.
11. Blackwell, L. J., and Borowiec, J. A. (1994) Human replication protein A binds single-stranded DNA in two distinct complexes. *Mol. Cell. Biol. 14*, 3993–4001.
12. Grudic, A., Jul-Larsen, Å., Haring, S. J., Wold, M. S., Lønning, P. E., Bjerkvij, R., and Bøe, S. O. (2007) Replication protein A prevents accumulation of single-stranded telomeric DNA in cells that use alternative lengthening of telomeres. *Nucleic Acids Res. 35*, 7267–7278.
13. Smith, J., Zou, H., and Rothstein, R. (2000) Characterization of genetic interactions with RFA1: The role of RPA in DNA replication and telomere maintenance. *Biochimie 82*, 71–78.
14. Schramke, V., Luciano, P., Brevet, V., Guillot, S., Corda, Y., Longhese, M. P., Gilson, E., and Géli, V. (2004) RPA regulates telomerase action by providing Est1p access to chromosome ends. *Nat. Genet. 36*, 46–54.
15. Croy, J. E., and Wuttke, D. S. (2006) Themes in ssDNA recognition by telomere-end protection proteins. *Trends Biochem. Sci. 31*, 516–525.
16. Gao, H., Cervantes, R. B., Mandell, E. K., Otero, J. H., and Lundblad, V. (2007) RPA-like proteins mediate yeast telomere function. *Nat. Struct. Mol. Biol. 14*, 208–214.
17. Hockemeyer, D., Palm, W., Else, T., Daniels, J. P., Takai, K. K., Ye, J. Z. S., Keegan, C. E., deLange, T., and Hammer, G. D. (2007) Telomere protection by mammalian Pot1 requires interaction with Tpp1. *Nat. Struct. Mol. Biol. 14*, 754–761.
18. Eldridge, A. M., and Wuttke, D. S. (2008) Probing the mechanism of recognition of ssDNA by the Cdc13-DBD. *Nucleic Acids Res. 36*, 1624–1633.
19. Burge, S., Parkinson, G. N., Hazel, P., Todd, A. K., and Neidle, S. (2006) Quadruplex DNA: Sequence, topology and structure. *Nucleic Acids Res. 34*, 5402–5415.
20. Salas, T. R., Petruseva, I., Lavrik, O., Bourdoncle, A., Mergny, J. L., Favre, A., and Saintomé, C. (2006) Human replication protein A unfolds telomeric G-quadruplexes. *Nucleic Acids Res. 34*, 4857–4865.
21. Wu, Y., Rawtani, N., Thazhathveetil, A. K., Kenny, M. K., Seidman, M. M., and Brosh, R. M., Jr. (2008) Human replication protein A melts a DNA triple helix structure in a potent and specific manner. *Biochemistry 47*, 5068–5077.
22. Pestryakov, P. E., Khlimankov, D. Y., Bochkareva, E., Bochkarev, A., and Lavrik, O. I. (2004) Human replication protein A (RPA) binds a primer-template junction in the absence of its major ssDNA-binding domains. *Nucleic Acids Res. 32*, 1894–1903.
23. Wen, J. D., and Gray, D. M. (2002) The Ff gene 5 single-stranded DNA-binding protein binds to the transiently folded form of an intramolecular G-quadruplex. *Biochemistry 41*, 11438–11448.
24. Gray, D. M., Wen, J. D., Gray, C. W., Repges, R., Repges, C., Raabe, G., and Fleischhauer, J. (2008) Measured and calculated CD spectra of G-quartets stacked with the same or opposite polarities. *Chirality 20*, 431–440.
25. Wen, J. D., Gray, C. W., and Gray, D. M. (2001) SELEX selection of high-affinity oligonucleotides for bacteriophage ff gene 5 protein. *Biochemistry 40*, 9300–9310.
26. Gray, D. M., Hung, S.-H., and Johnson, K. H. (1995) Absorption and circular dichroism spectroscopy of nucleic acid duplexes and triplexes. *Methods Enzymol. 246*, 19–34.
27. Bochkareva, E., Frappier, L., Edwards, A. M., and Bochkarev, A. (1998) The RPA32 subunit of human replication protein A contains a single-stranded DNA-binding domain. *J. Biol. Chem. 273*, 3932–3936.
28. Pfuetzner, R. A., Bochkarev, A., Frappier, L., and Edwards, A. M. (1997) Replication protein A. Characterization and crystallization of the DNA binding domain. *J. Biol. Chem. 272*, 430–434.
29. Weber, K., and Osborn, M. (1969) The reliability of molecular weight determinations by dodecyl sulfate-polyacrylamide gel electrophoresis. *J. Biol. Chem. 244*, 4406–4412.
30. Pace, C. N., Vajdos, F., Fee, L., Grimsley, G., and Gray, T. (1995) How to measure and predict the molar absorption coefficient of a protein. *Protein Sci. 4*, 2411–2423.
31. Savitzky, A., and Golay, M. J. E. (1964) Smoothing and Differentiation of Data by Simplified Least Squares Procedures. *Anal. Chem. 36*, 1627–1639.
32. Sreerama, N., Venyaminov, S. Y., and Woody, R. W. (2000) Estimation of protein secondary structure from circular dichroism spectra: Inclusion of denatured proteins with native proteins in the analysis. *Anal. Biochem. 287*, 243–251.
33. Sreerama, N., and Woody, R. W. (2000) Estimation of protein secondary structure from circular dichroism spectra: Comparison of CONTIN, SELCON, and CDSSTR methods with an expanded reference set. *Anal. Biochem. 287*, 252–260.
34. Kabsch, W., and Sander, C. (1983) Dictionary of protein secondary structure: Pattern recognition of hydrogen-bonded and geometrical features. *Biopolymers 22*, 2577–2637.
35. Bochkareva, E., Belegu, V., Korolev, S., and Bochkarev, A. (2001) Structure of the major single-stranded DNA-binding domain of replication protein A suggests a dynamic mechanism for DNA binding. *EMBO J. 20*, 612–618.
36. Bochkareva, E., Korolev, S., Lees-Miller, S. P., and Bochkarev, A. (2002) Structure of the RPA trimerization core and its role in the multistep DNA-binding mechanism of RPA. *EMBO J. 21*, 1855–1863.
37. Bochkareva, E., Kaustov, L., Ayed, A., Yi, G. S., Lu, Y., Pineda-Lucena, A., Liao, J. C. C., Okorokov, A. L., Milner, J., Arrowsmith, C. H., and Bochkarev, A. (2005) Single-stranded DNA mimicry in the p53 transactivation domain interaction with replication protein A. *Proc. Natl. Acad. Sci. U.S.A. 102*, 15412–15417.
38. Nuss, J. E., and Alter, G. M. (2004) Denaturation of replication protein A reveals an alternative conformation with intact domain structure and oligonucleotide binding activity. *Protein Sci. 13*, 1365–1378.
39. Wyka, I. M., Dhar, K., Binz, S. K., and Wold, M. S. (2003) Replication protein A interactions with DNA: Differential binding of the core domains and analysis of the DNA interaction surface. *Biochemistry 42*, 12909–12918.
40. Tuerk, C., and Gold, L. (1990) Systematic evolution of ligands by exponential enrichment: RNA ligands to bacteriophage T4 DNA polymerase. *Science 249*, 505–510.
41. Schneider, D. J., Feigon, J., Hostomsky, Z., and Gold, L. (1995) High-affinity ssDNA inhibitors of the reverse transcriptase of type 1 human immunodeficiency virus. *Biochemistry 34*, 9599–9610.
42. Mou, T. C., Shen, M., Abdalla, S., Delamora, D., Bochkareva, E., Bochkarev, A., and Gray, D. M. (2006) Effects of ssDNA sequences on non-sequence-specific protein binding. *Chirality 18*, 370–382.
43. Gottarelli, G., Masiero, S., and Spada, G. P. (1998) The use of CD spectroscopy for the study of the self-assembly of guanine derivatives. *Enantiomer 3*, 429–498.
44. Gray, D. M. (2000) CD of Protein-Nucleic Acid Interactions. In *Circular Dichroism: Principles and Applications* (Berova, N.,

Nakanishi, K., and Woody, R. W., Eds.) 2nd ed., pp 769−796, John Wiley & Sons, New York.
45. Mathews, D. H., Disney, M. D., Childs, J. L., Schroeder, S. J., Zuker, M., and Turner, D. H. (2004) Incorporating chemical modification constraints into a dynamic programming algorithm for prediction of RNA secondary structure. *Proc. Natl. Acad. Sci. U.S.A. 101*, 7287–7292.
46. Mou, T.-C., Gray, C. W., and Gray, D. M. (1999) The binding affinity of Ff gene 5 protein depends on the nearest-neighbor composition of the ssDNA substrate. *Biophys. J. 76*, 1637–1551.
47. Bochkareva, E., Korolev, S., and Bochkarev, A. (2000) The role for zinc in replication protein A. *J. Biol. Chem. 275*, 27332–27338.
48. Kim, C., Paulus, B. F., and Wold, M. S. (1994) Interactions of human replication protein A with oligonucleotides. *Biochemistry 33*, 14197–14206.
49. Kumaran, S., Kozlov, A., and Lohman, T. M. (2006) *Saccharomyces cerevisiae* replication protein A binds to single-stranded DNA in multiple salt-dependent modes. *Biochemistry 45*, 11958–11973.
50. Qin, Y., and Hurley, L. H. (2008) Structures, folding patterns, and functions of intramolecular DNA G-quadruplexes found in eukaryotic promoter regions. *Biochimie 90*, 1149–1171.
51. Granotier, C., Pennarun, G., Riou, L., Hoffschir, F., Gauthier, L. R., Cian, A. D., Gomez, D., Mandine, E., Riou, J.-F., Mergny, J.-L., Mailliet, P., Dutrillaux, B., and Boussin, F. D. (2005) Preferential binding of a G-quadruplex ligand to human chromosome ends. *Nucleic Acids Res. 33*, 4182–4190.

BI801538H